

Measurement of Branching Fraction of $B^- \rightarrow D^0\pi^-\pi^+\pi^-$

Shubhajit Sana

Roll: PH18B004

Guide: Prof. James F. Libby



Department of Physics,
Indian Institute of Technology Madras,
Chennai 600036, India

November 22, 2022



Outline

- 1 SuperKEKB Accelerator
- 2 Belle II detector
- 3 Full Event Interpretation
- 4 Motivation
- 5 Analysis

SuperKEKB accelerator



- Super KEKB: 4 GeV e^+ and 7 GeV e^- asymmetric collider at KEK, Japan.
 - 3 km circumference and 41 mrad crossing angle.
 - The center-of-mass energy is close to the mass of $\Upsilon(4S)$, which decays later to $B\bar{B}$ pair.
 - A 30-fold increase in Luminosity over Belle, $L = 6 \times 10^{35} \text{ cm}^{-2} \text{ s}^{-1}$.
 - Uses the nano-beam scheme (minimization of vertical beta function); hence doubled current.
 - Better performance and can tolerate the much higher level of beam-related backgrounds due to the increase in instantaneous luminosity.
 - **Belle II detector** is at the interaction point.

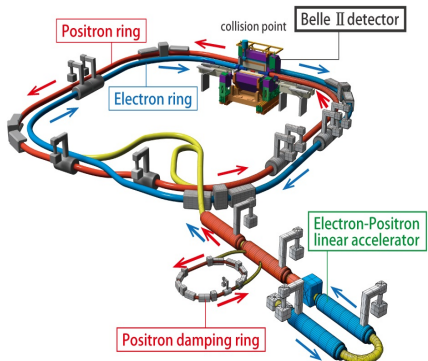


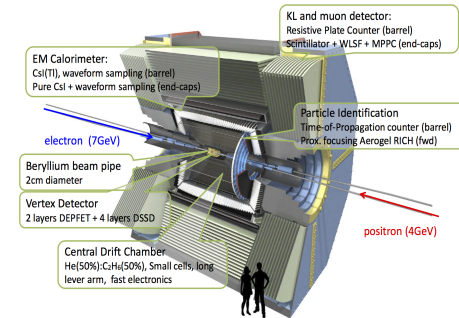
Figure: SuperKEKB accelerator



Belle II detector

- Vertex detector (PXD+SVD): two layers of pixel detector and four layers of SVD to determine B meson decay vertices.
 - Central drift chamber (CDC): A large gaseous detector that acts as the principal tracking device.
 - Aerogel Ring Imaging Cherenkov Counter (ARICH): Used for particle identification, mainly to distinguish between pions and kaons.
 - Time-of-Propagation Counters (TOP): Cerenkov radiation totally internally reflected within quartz bars for particle identification.
 - Electromagnetic calorimeter (ECAL): Detects photons and measures their energy and position with thallium-doped caesium iodide crystals.

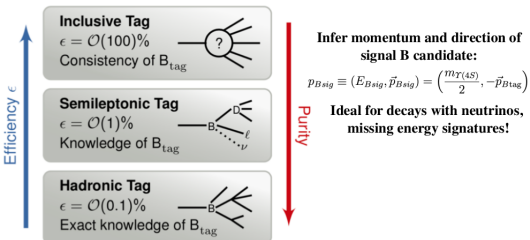
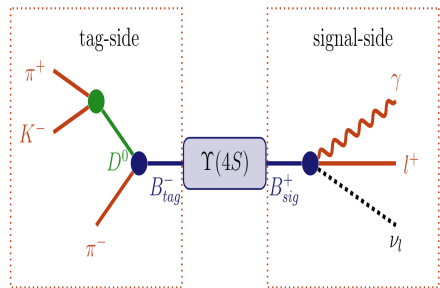
Belle II Detector



- K-Long and muon detector (KLM): Detects muons and long-lived neutral kaons, and distinguishes between them using scintillators along with RPCs.
 - Superconducting Solenoid : Provides a homogeneous magnetic field of 1.5T along the beam axis.

Full Event Interpretation

- Implement tagging, where one B referred to as B_{tag} is exclusively reconstructed using hadronic or semi-leptonic modes.
- The remaining tracks and clusters are then attributed to B_{sig} , on which the search or measurement of a particular decay is done.
- Any missing energy is attributed to the B_{sig} .



Full Event Interpretation

- Final-state particle candidates are selected and corresponding classification methods are trained using the detector information.
- Intermediate particle candidates are reconstructed and a multivariate classifier is trained for each employed decay channel.
- Employs over 200 Boosted Decision Trees to reconstruct more than 10000 B decay modes.

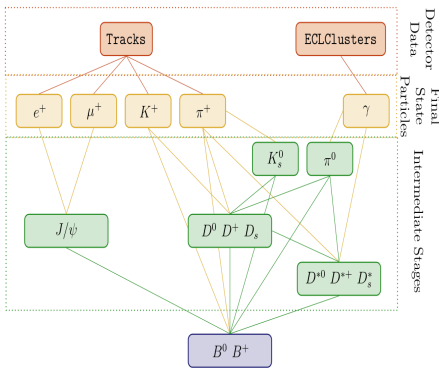
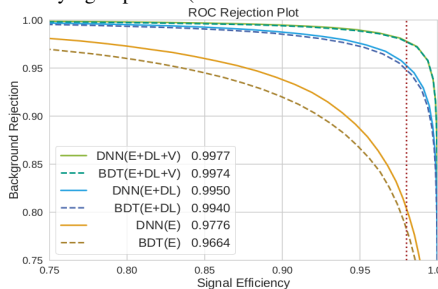


Figure: MVC algorithm with Hierarchical approach

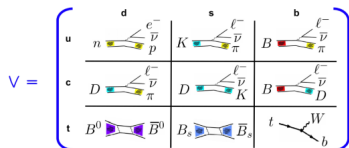
Boosted Decesion Tree

- Boosted Decision Trees (BDTs) are a specific type of a machine learning model used for classification tasks.
- The name decision tree refers to the general structure: the classification is done with a series of “decisions”.
- Decisions are logical operations (like “>”, “<”, “=”, etc.) on the input variables of each data point, by the outcome of which the data points are separated into groups.
- The word boosted refers to the specific way the tree is formed: gradient boosting. Gradient boosting means, that a final tree is made by combining a series of smaller trees of a fixed depth.
- The BDT is a supervised machine learning method, i.e. it needs to be trained on a dataset where we know the true class that we are trying to predict (this variable is called the target variable).
- FastBDT is the fastest contestant for small models (depth of the trees <5 and number of trees <300), whereas XGBoost has a slightly better scaling behaviour for large models.
- Used in FEI and to reject continuum background.



Motivation

- Inclusive and exclusive $b \rightarrow ulv$ and $b \rightarrow clv$ transitions are crucial for the determination of the CKM matrix elements $|V_{ub}|$ and $|V_{cb}|$.



- FEI is a powerful technique to reconstruct such decays with missing energy.
- Tag decays include high branching fraction decays like $B^- \rightarrow D^0 \pi^- \pi^+ \pi^-$.

$$\text{BF} = (5.6 \pm 2.1) \times 10^{-3}$$

- However it is not well simulated in MC because of the large uncertainty on the branching fraction.
- Goal is to improve the accuracy of the branching fraction measurement of $B^- \rightarrow D^0 \pi^- \pi^+ \pi^-$.

Selection Cuts

- Data Set: MC15ri_a inclusive MC (200 fb^{-1})

- **Object selection:**

- ▶ Transverse impact parameter $|d_0| < 0.2 \text{ cm}$.
- ▶ Longitudinal impact parameter $|z_0| < 1 \text{ cm}$.
- ▶ Polar angle $\rightarrow 0 < \theta < 126.87$: $\cos \theta \geq -0.6$

- Selection on kinematic variables:

- ▶ Mass of D^0 meson: $1.84 < M < 1.89 \text{ GeV}/c^2$
- ▶ Beam constrained mass $5.23 \text{ GeV}/c^2 < (M_{bc}) < 5.29 \text{ GeV}/c^2$, defined as
$$M_{bc} = \sqrt{E_{\text{beam}}^2 - (\sum \vec{p}_i)^2}.$$
- ▶ Beam-energy Difference $|\Delta E| < 0.1 \text{ GeV}$, defined as $\Delta E = \sum E_i - E_{\text{beam}}$.

Plotting M_{bc}

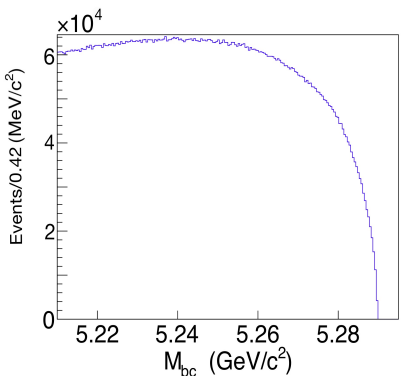


Figure: For background

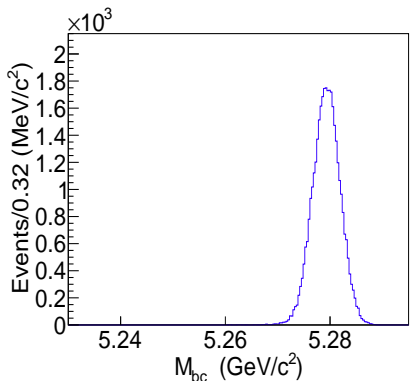


Figure: For Truth Matched(TM)
events

Plotting ΔE

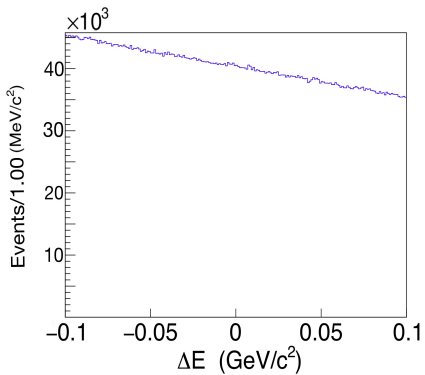


Figure: For background

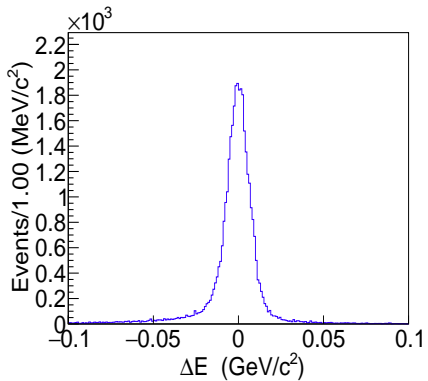


Figure: For Truth Matched(TM) events

$\mathcal{L}(K \mid \pi)$

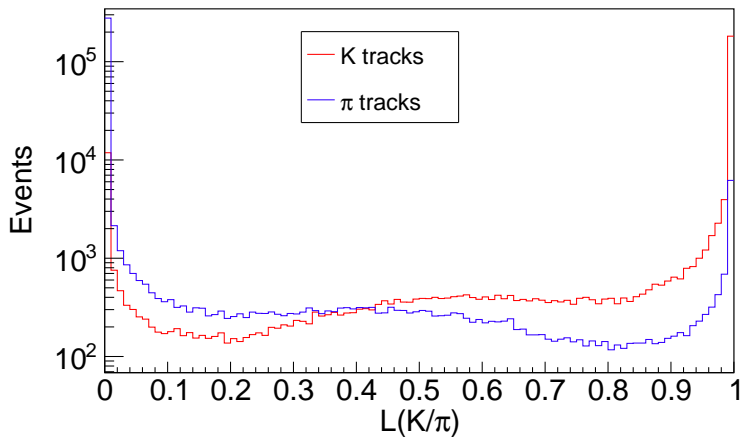


Figure: Distribution of $\mathcal{L}(K \mid \pi)$ for charged kaon and pion tracks in the signal MC sample.

Figure of Merit

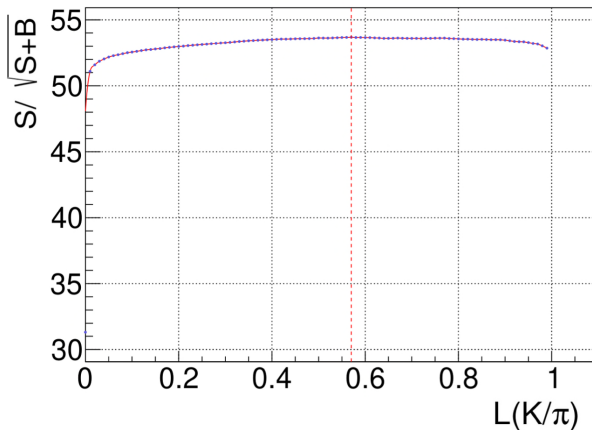


Figure: Distribution of $S/\sqrt{S+B}$ for PID selection optimization for kaon tracks originating from \bar{D}^0



Selection Cuts

● Object selection:

- ▶ Transverse impact parameter $|d_0| < 0.2$ cm.
- ▶ Longitudinal impact parameter $|z_0| < 1$ cm.
- ▶ Polar angle $\rightarrow 0 < \theta < 126.87$: $\cos \theta >= -0.6$.
- ▶ **Binary likelihood, $\mathcal{L}(K | \pi) > 0.6$.**

● Selection on kinematic variables:

- ▶ Mass of D^0 meson: $1.84 < M < 1.89$ GeV/c 2
- ▶ Beam constrained mass 5.23 GeV/c $^2 < (M_{bc}) < 5.29$ GeV/c 2 , defined as
$$M_{bc} = \sqrt{E_{\text{beam}}^2 - (\sum \vec{p}_i)^2}$$
.
- ▶ Beam-energy Difference $|\Delta E| < 0.1$ GeV, defined as $\Delta E = \Sigma E_i - E_{\text{beam}}$.

Mass of \bar{D}^0

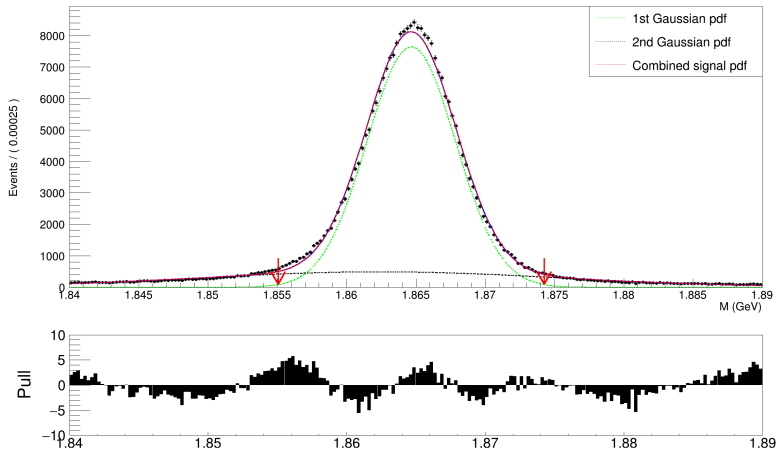


Figure: Fitting invariant mass of daughter particles (K^+, π^-) of \bar{D}^0



Selection Cuts

● Object selection:

- ▶ Transverse impact parameter $|d_0| < 0.2$ cm.
- ▶ Longitudinal impact parameter $|z_0| < 1$ cm.
- ▶ Polar angle $\rightarrow 0 < \theta < 126.87$: $\cos \theta >= -0.6$.
- ▶ Binary likelihood, $\mathcal{L}(K | \pi) > 0.6$.

● Selection on kinematic variables:

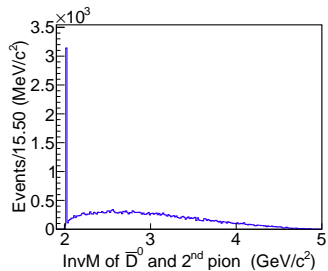
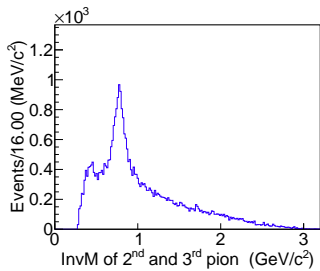
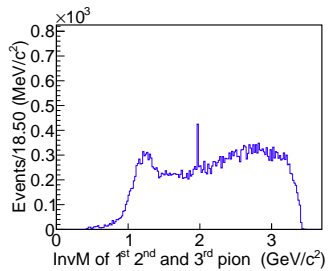
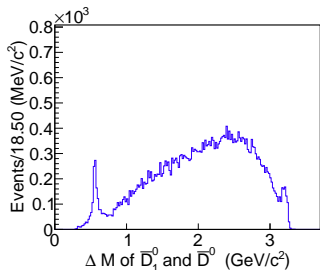
- ▶ Mass of D^0 meson: $1.855 < M < 1.874$ GeV/c².
- ▶ Beam constrained mass 5.23 GeV/c² $< (M_{bc}) < 5.29$ GeV/c², defined as
$$M_{bc} = \sqrt{E_{\text{beam}}^2 - (\sum \vec{p}_i)^2}$$
.
- ▶ Beam-energy Difference $|\Delta E| < 0.1$ GeV, defined as $\Delta E = \Sigma E_i - E_{\text{beam}}$.



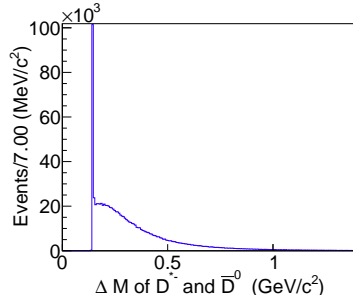
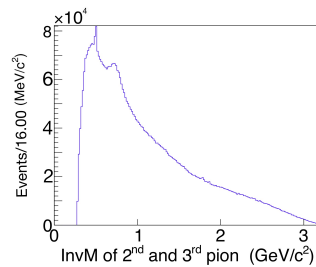
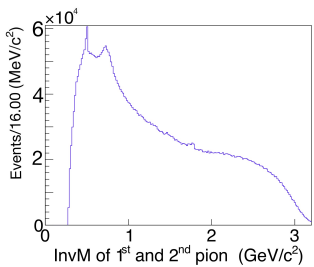
Topological analysis of TM events

rowNo	exclusive component of $B^+ \rightarrow \pi^+\pi^+\pi^-\bar{D}^0$	iDcyBrIRADcyBr	nCase	nCcCase	nAllCase	nCCase
1	$B^+ \rightarrow \pi^+\pi^+\pi^-\bar{D}^0$	2	4717	4400	9117	9117
2	$B^+ \rightarrow \rho^0\pi^+\bar{D}^0, \rho^0 \rightarrow \pi^+\pi^-$	0	4339	4264	8603	17720
3	$B^+ \rightarrow \bar{D}^0 a_1^+, a_1^+ \rightarrow \rho^0\pi^+, \rho^0 \rightarrow \pi^+\pi^-$	1	1689	1785	3474	21194
4	$B^+ \rightarrow \bar{D}^0 a_1^+, a_1^+ \rightarrow \pi^+\pi^+\pi^-$	7	744	781	1525	22719
5	$B^+ \rightarrow \bar{D}^0 a_1^+, a_1^+ \rightarrow \pi^+ f_0(600), f_0(600) \rightarrow \pi^+\pi^-$	5	629	592	1221	23940
6	$B^+ \rightarrow \pi^+\pi^+D^{*-}, D^{*-} \rightarrow \pi^-\bar{D}^0$	3	509	501	1010	24950
7	$B^+ \rightarrow \pi^+\bar{D}_1^0, \bar{D}_1^0 \rightarrow \pi^+\pi^-\bar{D}^0$	14	233	226	459	25409
8	$B^+ \rightarrow \pi^+\bar{D}_1^0, \bar{D}_1^0 \rightarrow \pi^+D^{*-}, D^{*-} \rightarrow \pi^-\bar{D}^0$	9	139	133	272	25681
9	$B^+ \rightarrow \pi^+\bar{D}_1^0, \bar{D}_1^0 \rightarrow \pi^+D^{*-}, D^{*-} \rightarrow \pi^-\bar{D}^0$	12	131	137	268	25949
10	$B^+ \rightarrow \pi^+\eta\bar{D}^0, \eta \rightarrow \pi^+\pi^-$	4	107	107	214	26163
11	$B^+ \rightarrow \bar{D}^0 D_s^+, D_s^+ \rightarrow \pi^+\pi^+\pi^-$	11	102	109	211	26374
12	$B^+ \rightarrow \pi^+\omega\bar{D}^0, \omega \rightarrow \pi^+\pi^-$	16	59	67	126	26500
13	$B^+ \rightarrow K^{*+}\bar{D}^0, K^{*+} \rightarrow \pi^+K^0, K^0 \rightarrow K_S^0, K_S^0 \rightarrow \pi^+\pi^-$	15	70	47	117	26617
14	$B^+ \rightarrow \pi^+\bar{D}_2^0, \bar{D}_2^0 \rightarrow \pi^+D^{*-}, D^{*-} \rightarrow \pi^-\bar{D}^0$	6	33	45	78	26695
15	$B^+ \rightarrow \bar{D}^0 a_1^+, a_1^+ \rightarrow \pi^+\rho^0(1450), \rho^0(1450) \rightarrow \pi^+\pi^-$	8	15	32	47	26742
16	$B^+ \rightarrow \pi^+K^0\bar{D}^0, K^0 \rightarrow K_S^0, K_S^0 \rightarrow \pi^+\pi^-$	13	22	8	30	26772
17	$B^+ \rightarrow \bar{D}^0 D_s^+, D_s^+ \rightarrow \pi^+\eta, \eta \rightarrow \pi^+\pi^-$	19	4	7	11	26783
18	$B^+ \rightarrow D^+\bar{D}^0, D^+ \rightarrow \pi^+K_S^0, K_S^0 \rightarrow \pi^+\pi^-$	17	4	2	6	26789
19	$B^+ \rightarrow \bar{D}^0 D_s^+, D_s^+ \rightarrow \pi^+K_S^0, K_S^0 \rightarrow \pi^+\pi^-$	18	1	4	5	26794
20	$B^+ \rightarrow \bar{D}^0 D_s^+, D_s^+ \rightarrow \pi^+\omega, \omega \rightarrow \pi^+\pi^-$	10	2	0	2	26796
rest	$B^+ \rightarrow \text{others (3 in total)} \rightarrow \pi^+\pi^+\pi^-\bar{D}^0$	—	3	0	3	26799

Distribution of the invariant mass



Distribution of the invariant mass



Different veto cuts and their efficiencies

- **Object selection:**

- ▶ Transverse impact parameter $|d0| < 0.2$ cm.
- ▶ Longitudinal impact parameter $|z0| < 1$ cm.
- ▶ Polar angle $\rightarrow 0 < \theta < 126.87$: $\cos \theta >= -0.6$.
- ▶ Binary likelihood, $\mathcal{L}(K | \pi) > 0.6$.

- Selection on kinematic variables:

- ▶ Mass of D^0 meson: $1.855 < M < 1.874$ GeV/c 2 .
- ▶ Beam constrained mass 5.27 GeV/c 2 $< (M_{bc}) < 5.29$ GeV/c 2 , defined as

$$M_{bc} = \sqrt{E_{\text{beam}}^2 - (\sum \vec{p}_i)^2}$$
.
- ▶ Beam-energy Difference $|\Delta E| < 0.1$ GeV, defined as $\Delta E = \sum E_i - E_{\text{beam}}$.

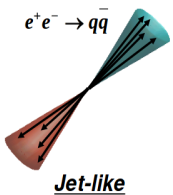
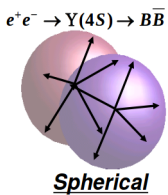
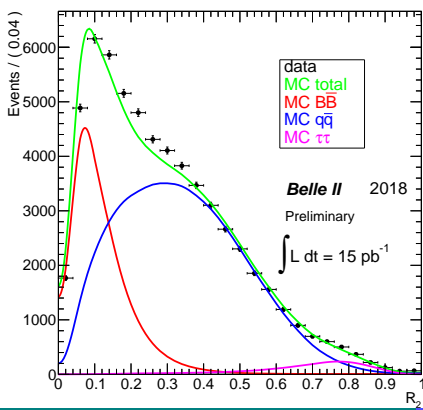
Variable name	Veto region (GeV/c 2)	Efficiency (%)
Invariant mass of three charged π	(1.95769 - 1.97872)	98.52
Invariant mass of one charged π and \bar{D}^0	(2.00837 - 2.01217)	91.35
Mass difference of \bar{D}_1^0 and \bar{D}^0	(0.492200 - 0.632197)	96.75
Invariant mass of two oppositely charged π (1 st and 2 nd)	(0.488814 - 0.506173)	99.08
Invariant mass of two oppositely charged π (2 nd and 3 rd)	(0.48987 - 0.504896)	98.83
Mass difference of D^{*-} and \bar{D}^0	(0.143913 - 0.146967)	97.32

Continuum Suppression

- R_2 : Ratio of second and zeroth Fox-Wolfram moment.

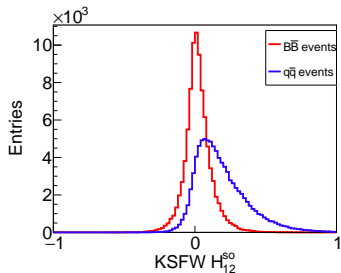
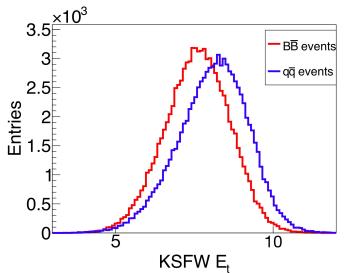
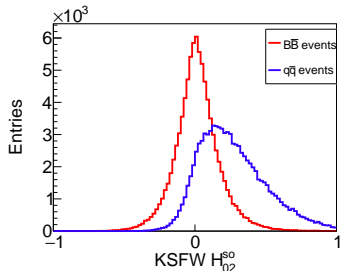
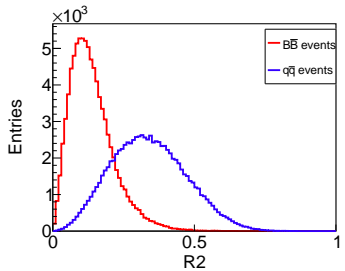
$$H_I = \sum_{ij} |p_i||p_j| P_I(\cos\theta_{ij})$$

i, j = charged & γ
 Momentum of particle i and j
 Legendre polynomial
 Angle between particle i and j

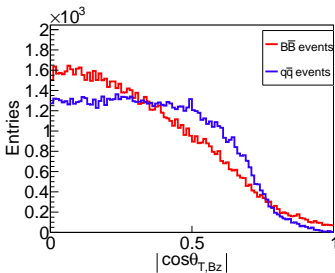
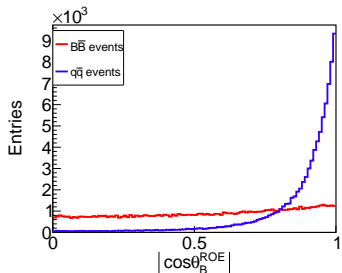
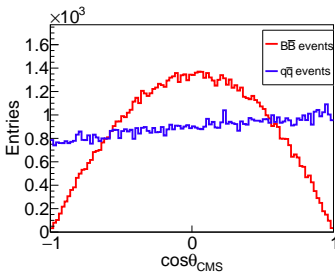
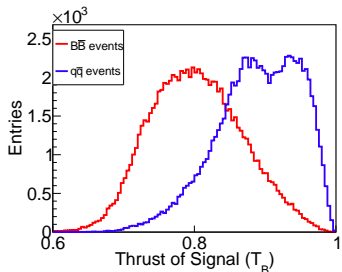


- Spherical limit: $R_2 \rightarrow 0$; jet-like limit: $R_2 \rightarrow 1$.
- So we are on $\Upsilon(4S)$ resonance and recording $B\bar{B}$ pairs.

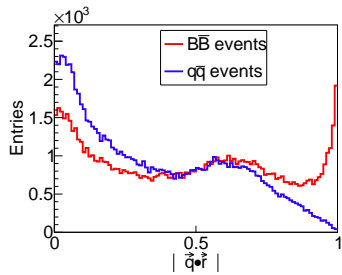
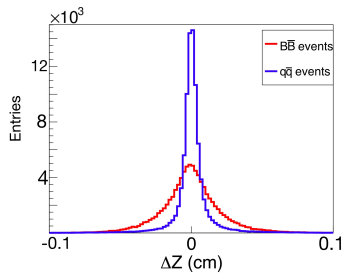
Distribution of R2, H_{02}^{so} , E_t and H_{12}^{so}



$|\cos \theta_{T,Bz}|$

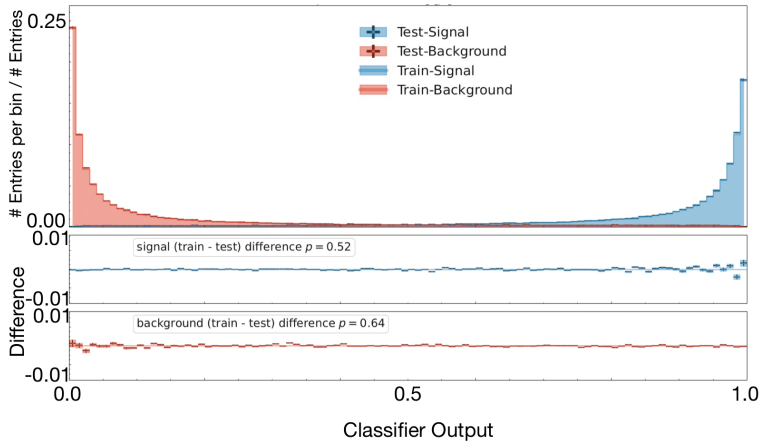


Distribution of Δz and $|q \cdot r|$



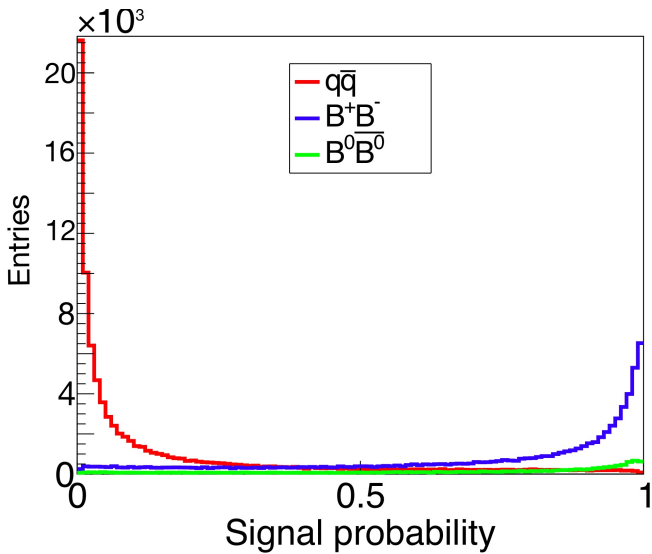


Overtraining plot



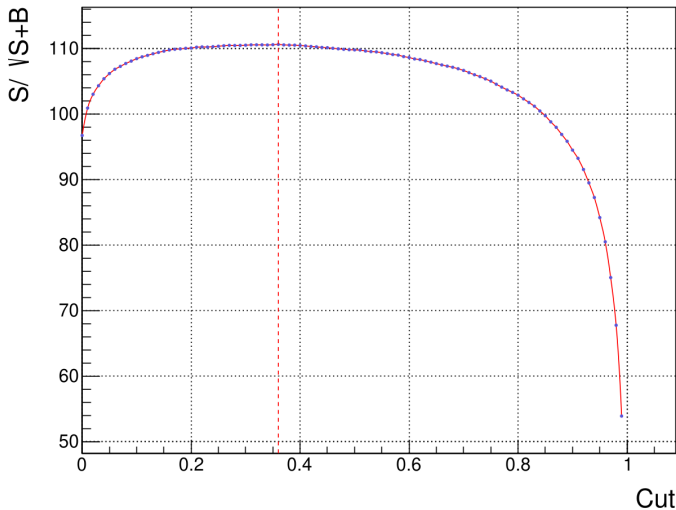


Classifier output





FoM analysis of FBDT output



Selection cuts

- Object selection:

- ▶ Transverse impact parameter $|d0| < 0.2$ cm.
- ▶ Longitudinal impact parameter $|z0| < 1$ cm.
- ▶ Polar angle $\rightarrow 0 < \theta < 126.87$: $\cos \theta >= -0.6$.
- ▶ Binary likelihood, $\mathcal{L}(K | \pi) > 0.6$.

- Selection on kinematic variables:

- ▶ Mass of D^0 meson: $1.855 < M < 1.874$ GeV/c 2 .
- ▶ Beam constrained mass 5.27 GeV/c $^2 < (M_{bc}) < 5.29$ GeV/c 2 , defined as

$$M_{bc} = \sqrt{E_{\text{beam}}^2 - (\sum \vec{p}_i)^2}$$
.
- ▶ Beam-energy Difference $|\Delta E| < 0.1$ GeV, defined as $\Delta E = \sum E_i - E_{\text{beam}}$.

- Selection on Classifier output:

- ▶ **Classifier output(C) > 0.36.**

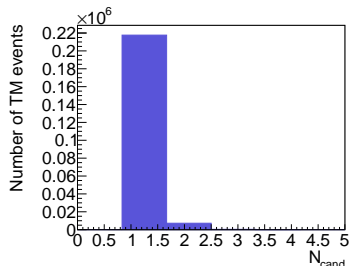
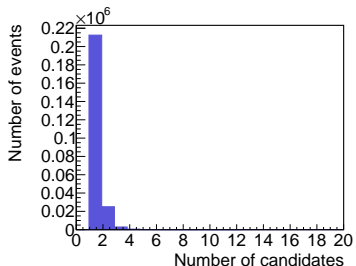
Variable name	Veto region (GeV/c 2)	Efficiency (%)
Invariant mass of three charged π	(1.95769 - 1.97872)	98.52
Invariant mass of one charged π and \bar{D}^0	(2.00837 - 2.01217)	91.35
Mass difference of \bar{D}_1^0 and \bar{D}^0	(0.492200 - 0.632197)	96.75
Invariant mass of two oppositely charged π (1 st and 2 nd)	(0.488814 - 0.506173)	99.08
Invariant mass of two oppositely charged π (2 nd and 3 rd)	(0.48987 - 0.504896)	98.83
Mass difference of D^{*-} and \bar{D}^0	(0.143913 - 0.146967)	97.32

Multiplicity distribution

- The χ^2 metric of M_{bc} and M_{D^0} , defined as

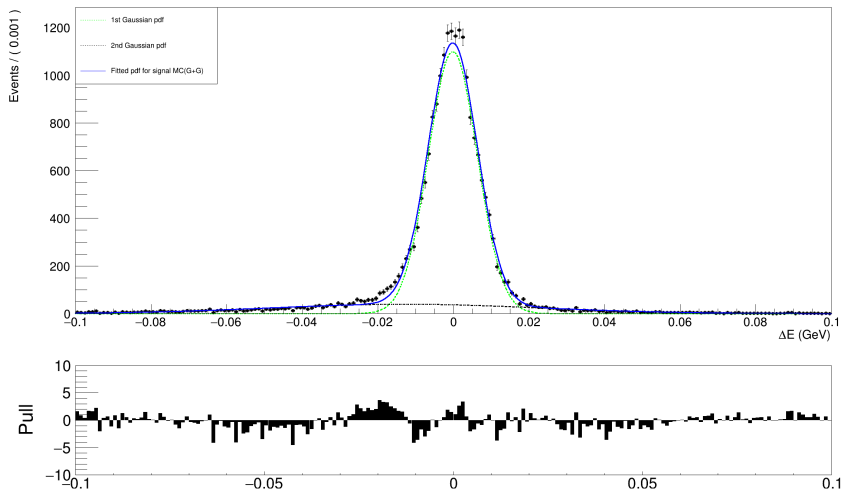
$$\left(\frac{M_{bc} - M_B^{\text{PDF}}}{\sigma_{M_{bc}}} \right)^2 + \left(\frac{M_{D^0} - M_{D^0}^{\text{PDF}}}{\sigma_{M_{D^0}}} \right)^2$$

is used for the single-candidate selection (SCS).

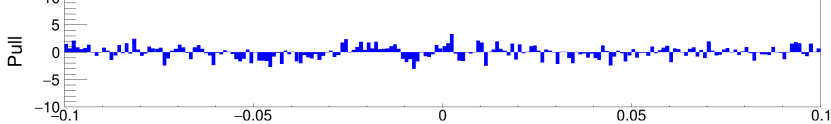
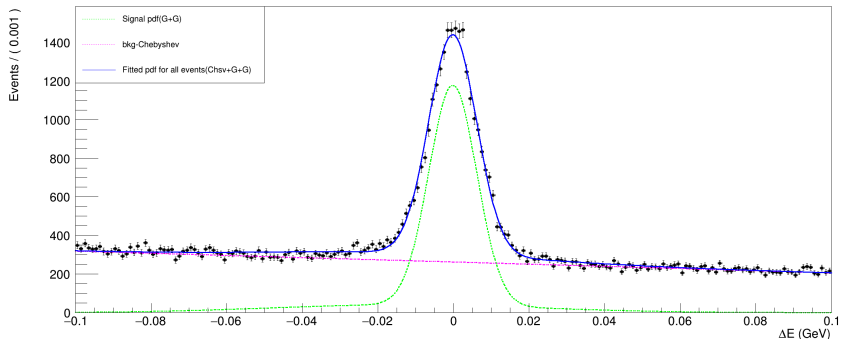


- The signal efficiencies obtained after applying all the selection criteria and single-candidate selection is **21.77%**.

Yield Measurement



Yield Measurement

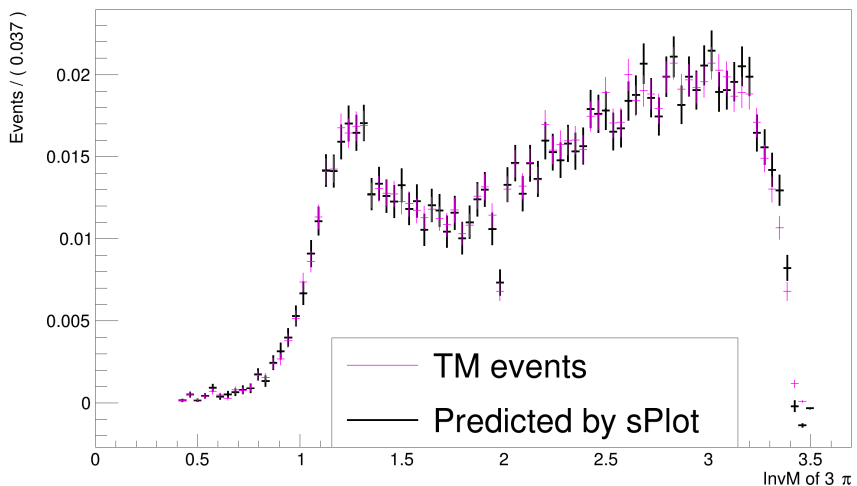


Results

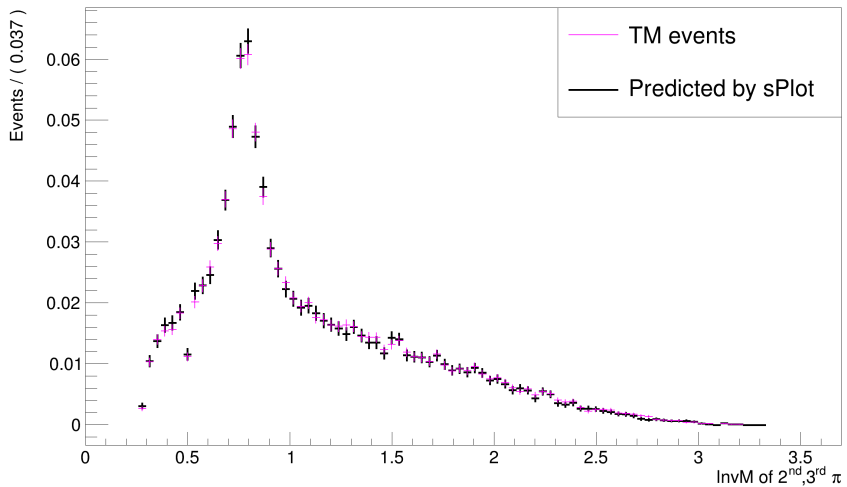
Component	Parameter	Value
Signal	μ_1	$(-0.175 \pm 0.054) \times 10^{-3}$ GeV
	μ_2	$(-12.61 \pm 0.68) \times 10^{-3}$ GeV
	σ_1	$(6.486 \pm 0.051) \times 10^{-3}$ GeV
	σ_2	$(35.79 \pm 0.60) \times 10^{-3}$ GeV
	f	0.836 ± 0.004
Background	b_0	-0.259 ± 0.010
Scale Factor	$f_{\Delta E}$	0.976 ± 0.009

- The yield of signal events was determined to be 21632 ± 207 .
- The measured value of the branching ratio for the decay channel $B^+ \rightarrow \bar{D}^0 \pi^+ \pi^- \pi^+$ is $(11.1 \pm 0.1) \times 10^{-3}$ which is consistent with the figure specified in the decay file used for the production of generic Monte Carlo (MC) data.

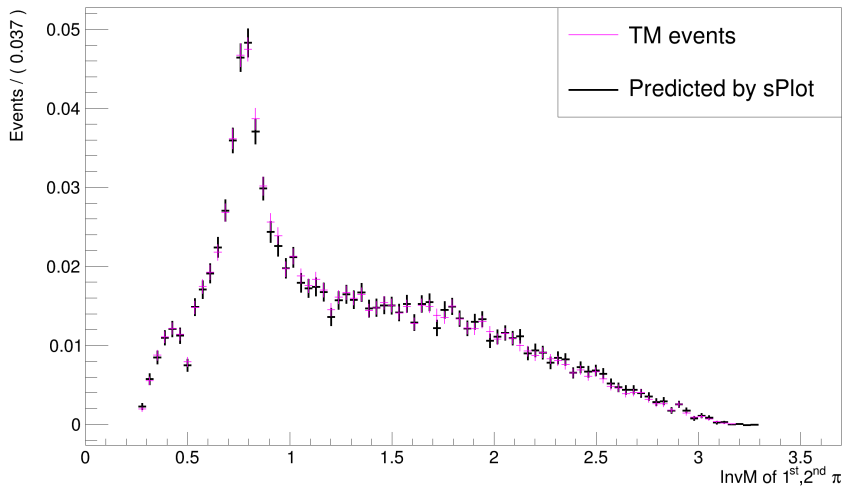
Predicted invariant mass from $sPlot$



Predicted invariant mass from $sPlot$



Predicted invariant mass from $sPlot$



SuperKEKB

FEI
000

Analysis

SuperKEKB

FEI
000

Analysis



Reference

- The Belle II Physics Book (KEK Preprint 2018-27)
- The Physics of the B Factories (KEK Preprint 2014-3)
- Observables for the Analysis of Event Shapes in e^+e^- Annihilation and Other Processes (1978)(7811220, CALT-688680)
- Belle II Software Documentation → software.belle2.org
- Root Data Analysis Framework user Guide → <https://root.cern/>

Thank you!

